Stabilization in finite time for a thermal system described by a parabolic partial differential equation in a 2D geometry

Sara Fakih, L. Perez, Laurent Autrique

Stabilization in finite time for a thermal system described by a parabolic partial differential equation in a 2D geometry

Sara FAKIH[1], Laetitia PEREZ[1], and Laurent AUTRIQUE[1]

***Abstract*— In thermal engineering, maintaining the temperature precisely at a desired setpoint is an essential objective for many processes. When heating actuators act locally and a few point sensors provide observations at different locations, the problem is complex. This communication deals with the control of a thermal system whose evolution is described by a parabolic partial differential equation (the domain is a thin steel plate subjected to heat sources on its upper surface, and to natural convection on its boundaries). The mathematical model remains valid in a 2D domain under the condition of negligible plate thickness. Equilibrium is reached when the combined effects of heat supplied by the sources and cooling induced by the surrounding environment balance out. The aim of this study is to achieve this state of equilibrium in a finite time by appropriately controlling the heat sources. The challenge of identifying these flows is addressed in the form of an inverse heat conduction problem (known to be ill-posed), and the implementation of the conjugate gradient regularization method is discussed.**

I. Introduction

Optimal control of systems described by partial differential equations (PDEs) remains a significant challenge, especially in the fields incorporating thermal sciences, where the precise manipulation of control inputs is crucial in achieving desired temperature outputs [3], [4], [6], [8]. The development of methods for synthesizing controllers is difficult for non-academic cases due to the need to address diverse complex requirements, while simultaneously aiming to balance thermal system performance. For example, ISS output feedback synthesis of disturbed reaction–diffusion processes using non-collocated sampled-in-space sensing and actuation is recently investigated in [7].

The motive behind this study lies in addressing the thermal scenario of a thin steel plate (characterized by its known material properties) in a two-dimensional geometry, where it is subjected to heating from four stationary disks along with natural convection across its surface. Nine pointwise sensors measure its temperature variation, and the equilibrium induced between the heating and cooling effects is considered the desired target temperature for these sensors. The primary objective is to achieve this stabilized state in a finite time by controlling the flux for each source, thus minimizing the cost function defined as the quadratic difference between the plate temperature and the desired target. This control problem can be easily formulated as a zero-stabilization problem, and the method developed in this context can be also implemented for compliance with a setpoint that varies in time and may be subjected to random disturbances. The range of applications is thus very broad.

The search for a control law is treated as an identification problem and formulated as an inverse one. In the context of inverse heat conduction, problems are ill-posed due to small perturbations on the observed states, leading to prohibitive errors on identified parameters [9]. In the specific framework of systems described by PDEs (linear or not), the Conjugate Gradient Method (CGM) is a powerful computational algorithm. The development of a global methodology based on its adaptation has garnered particular attention in various recent studies, including [1], [2], [5], [10], [11] and [12], for estimating unknown parameters such as physical properties, disturbances, and control laws in 1D domains. Required iterative steps are respectively outlined in the well-posed: direct problem - adjoint problem - sensitivity problem. Through this paper, CGM extends beyond parametric problems and control in 1D domains, providing an attractive approach for controller identification in 2D geometries. This numerical method provides a relevant and efficient approach in stabilizing complex processes in thermal engineering. Alongside fundamental research, often carried out in an academic context with sometimes reductive hypotheses, it is essential to develop constructive approaches based on robust numerical methods to synthesize control laws outside the framework of existing theories.

This document is structured as follows: notations and problem formulation are exposed in section II. Simulation results to achieve the target temperature are shown in section III. Developments related to the CGM implementation are detailed in section IV. An overview of the CGM algorithm is provided in section V. The CGM simulation results for the steel plate temperature stabilization in finite time are exposed in section VI. Concluding insights and perspectives are then proposed in section VII, offering valuable reflections on future research directions and potential applications.

II. Notations and direct problem formulation

Following notations are adopted in this paper: the spatial domain is a $1\ m^2$ squared steel plate $\Omega = [0,1]^2 \subset \mathbb{R}^2$, where the space variables are $(x, y) \in \Omega$ (each measured in m). It is important to notice that this is not an academic configuration: in our research institute, such plate will be soon employed in testing several configurations. In fact, setting its thickness as negligible, this study focuses on a $2D$ analysis. The boundary of Ω is $\Gamma \subset \mathbb{R}$, and the time

[1]Sara Fakih, Laetitia Perez and Laurent Autrique are with LARIS, Polytech, University of Angers, 62 avenue notre dame du lac, 49000, Angers, France. sara.fakih@univ-angers.fr laetitia.perez@univ-angers.fr laurent.autrique@univ-angers.fr

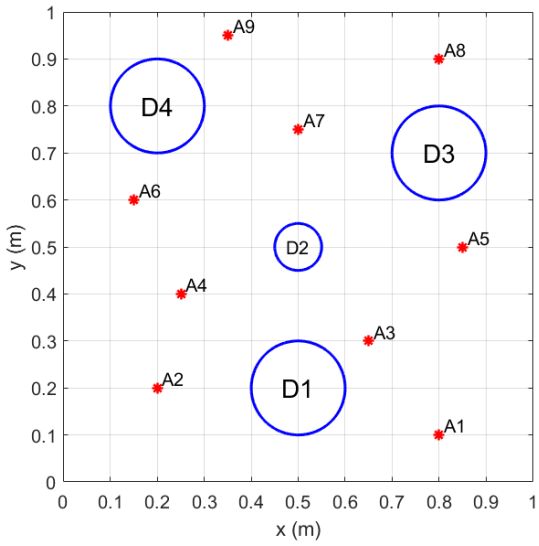

Fig. 1: Sensors and actuators locations.

variable (in s) is $t \in T = [0, t_f]$, where t_f is the final time. With the above indications, the temperature varying on $(x, y, t) \in \Omega \times T$ is denoted by $\theta(x, y, t)$ (in °C), and as in [12] work, its evolution is characterized by the following well-posed direct problem:

$$\rho C \frac{\partial \theta}{\partial t} - \lambda \Delta \theta = \frac{-h(\theta - \theta_0) + u(x, y)}{e} \quad \text{on } \Omega \times T \quad (1)$$

$$\theta(x, y, 0) = \theta_0(x, y) \quad \text{on } \Omega \quad (2)$$

where ρC is the volumetric heat capacity $(J.m^{-3}.K^{-1})$, λ is the thermal conductivity $(W.m^{-1}.K^{-1})$, $\Delta = \partial_x^2 + \partial_y^2$ is the Laplace operator, h is the convective heat transfer coefficient $(W.m^{-2}.K^{-1})$, $\theta_0(x, y)$ is the ambient temperature (°C), and $u(x, y)$ is the heating flux $(W.m^{-2})$. Homogeneous Neumann boundary condition exists on Γ:

$$-\lambda \frac{\partial \theta}{\partial \vec{n}} = 0 \quad \text{on } \Gamma \times T \quad (3)$$

where $\vec{n}$ is the outward unit normal vector on Γ. Heating stationary disks are defined as follows:

$$\mathcal{D}_1 = \{(x, y) \in \Omega;\ (x - 0.5)^2 + (y - 0.2)^2 \leq 0.1^2\}$$
$$\mathcal{D}_2 = \{(x, y) \in \Omega;\ (x - 0.5)^2 + (y - 0.5)^2 \leq 0.05^2\}$$
$$\mathcal{D}_3 = \{(x, y) \in \Omega;\ (x - 0.8)^2 + (y - 0.7)^2 \leq 0.1^2\}$$
$$\mathcal{D}_4 = \{(x, y) \in \Omega;\ (x - 0.2)^2 + (y - 0.8)^2 \leq 0.1^2\}$$

The heating flux is spatially constant on each disk and is denoted by u_i for $i = 1, \ldots, 4$. Thus:

$$u(x, y) = \sum_{i=1}^{4} u_i \mathbf{1}_{\mathcal{D}_i}(x, y)$$

where $\mathbf{1}_{\mathcal{D}_i}(x, y)$ is the indicator function (equal to 1 if $(x, y) \in \mathcal{D}_i$ and 0 elsewhere). Nine pointwise sensors A_i detecting temperature evolution are arbitrarily distributed in Ω (see table I and fig. 1).

TABLE I: Sensors locations

Sensor A_1	(0.8,0.1)	**Sensor** A_2	(0.2,0.2)
Sensor A_3	(0.65,0.3)	**Sensor** A_4	(0.25,0.4)
Sensor A_5	(0.85,0.5)	**Sensor** A_6	(0.15,0.6)
Sensor A_7	(0.5,0.75)	**Sensor** A_8	(0.8,0.9)
Sensor A_9	(0.35,0.95)		

III. Direct and control problems

A. *Direct problem simulation and desired target*

In table II, the steel plate material properties and other model input parameters are given.

TABLE II: Input parameters

Parameter	Value
Volumetric heat capacity	$\rho C = 2 \times 10^6\ J.m^{-3}.K^{-1}$
Thermal conductivity	$\lambda = 44\ W.m^{-1}.K^{-1}$
Convective heat transfer coefficient	$h = 10\ W.m^{-2}.K^{-1}$
Heating fluxes in $W.m^{-2}$	$u_1 = 4 \times 10^3$, $u_2 = 10^4$ $u_3 = 5 \times 10^3$, $u_4 = 6 \times 10^3$
Plate thickness	$e = 2 \times 10^{-3}\ m$
Initial temperature	$\theta_0(x, y) = 20$ °C
Final time	$t_f = 3600\ s$

Knowing $\{\rho, C, \lambda, h, u_1, u_2, u_3, u_4, e, \theta_0, t_f\}$, direct problem could be solved: find $\theta(x, y, t)$ solution of (1)-(3). This operation is carried out using the finite element method implemented with COMSOL Multiphysics and MATLAB. Temperature distribution is illustrated in fig. 2 and evolution for each sensor is shown in fig.3. One can observe from (fig. 2d) that after one hour, steady state is obtained. In what follows, this steady state is considered as the desired target.

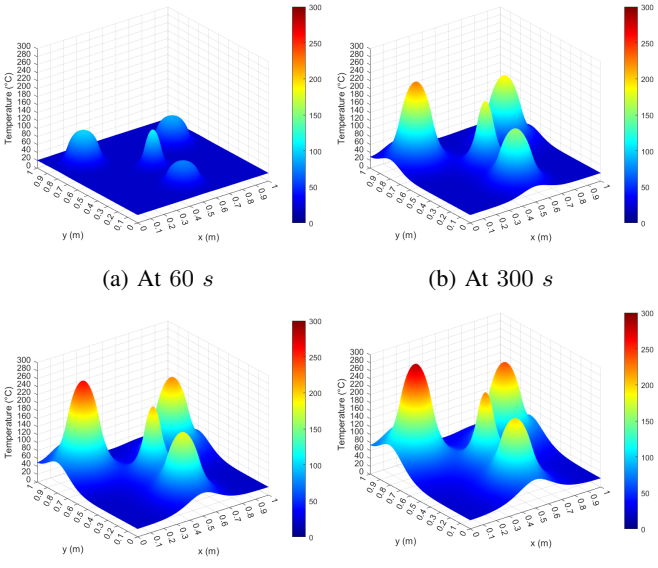

(a) At 60 s (b) At 300 s

(c) At 600 s (d) At 3600 s

Fig. 2: Temperature distribution for several times.

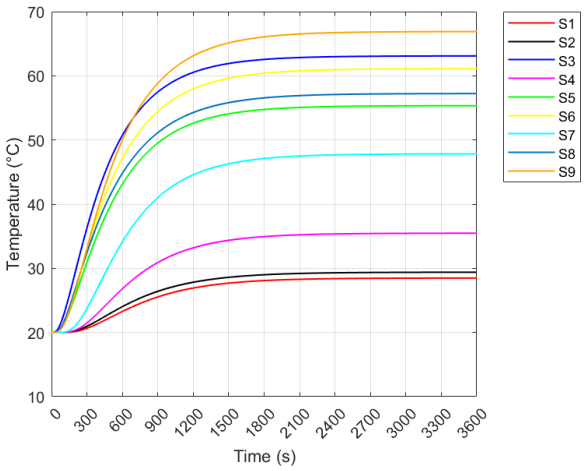

Fig. 3: Temperature evolution at S_i (Sensors A_i).

In fact, notate the following: $\theta(x, y, t_f) = \theta_{target}(x, y)$, for all $(x, y) \in \Omega$, and $\theta(A_i, t_f) = \theta_{target}(A_i)$, for $i = 1, \ldots, 9$.

B. *Control problem definition*

Figure 3 clearly highlights that in the last quarter of an hour, the temperature of each sensor is close to the desired target state. This is not the case in the first half-hour: the effect of the initial state (which can be considered here as a disturbance) is still perceptible.

In the following, the objective is to obtain the steady state earlier, i.e. in a reduced fixed time. Denote $t_f^* \in [0, 300]$ and define $T^* = [0, t_f^*]$. The control problem is employed in finding the control law (varying heating flux) $u(x, y, t)$ needed to achieve $\theta(A_i, t_f^*) \simeq \theta_{target}(A_i)$. This control is added to (1) instead of $u(x, y)$, and $\forall (x, y, t) \in \Omega \times T^*$:

$$u(x, y, t) = \sum_{i=1}^{4} u_i(t) \mathbf{1}_{\mathcal{D}_i}(x, y) \tag{4}$$

The objective is to identify the appropriate time-varying control laws $u_i(t)$, which are spatially constant on each corresponding disk $\mathcal{D}_i$ as defined in (4). Choosing $t_f^* = 300\ s$ serves a dual purpose because of the temperature's significant divergence at this time from the steady state, and as it allows sufficient time for the conduction phenomena from the controlled disks to the sensors A_i. Thus, the identified heating fluxes (controls) remain in a realistic range. In order to achieve thermal steady state for $\theta(A_i, t_f^*)$, the problem could be formulated as a stabilization to zero for $\psi(A_i, t_f^*)$. Indeed, for $(x, y, t) \in \Omega \times T^*$, define the error function:

$$\psi(x, y, t) = \theta(x, y, t) - \theta_{target}(x, y)$$

From (1)-(3), it can be easily verified that it is the solution of the following PDE on $\Omega \times T^*$:

$$\rho C \frac{\partial \psi}{\partial t} - \lambda \Delta \psi = \lambda \Delta \theta_{target} + \frac{-h(\psi - \psi_0) + u(x, y, t)}{e} \tag{5}$$

with the initial condition for $(x, y) \in \Omega$:

$$\psi(x, y, 0) = \psi_0(x, y) = \theta_0(x, y) - \theta_{target}(x, y) \tag{6}$$

and the Neumann boundary condition:

$$-\lambda \frac{\partial \psi}{\partial \vec{n}} = 0 \quad \text{on } \Gamma \times T^* \tag{7}$$

The inverse heat conduction problem dedicated in identifying the controls $\{u_i(t)\}_{i=1,\ldots,4}$ is solved in the next section considering the Conjugate Gradient Method (CGM).

IV. The Conjugate Gradient Method

A. *Formulation and notations*

The objective of CGM is to identify the control flux $u(x, y, t)$ in (4) required for minimizing the cost function (criterion) J defined at the final time $t_f^* = 300\ s$ as:

$$J(\psi; u) = \frac{1}{2} \sum_{i=1}^{9} \psi(A_i, t_f^*; u)^2 \tag{8}$$

where $\psi(x, y, t)$ satisfies (5)-(7) and sensors A_i locations are given in table I. For the implementation of CGM, each $\{u_i(t)\}_{i=1,\ldots,4}$ is discretized, without loss of generality, as a piecewise linear continuous function. For $i = 1, \ldots, 4$:

$$u_i(t) = \sum_{j=1}^{N_t} u_{ij} s_j(t) \tag{9}$$

where N_t is the number of time discretizations, and $u_{ij} = u_i(t_j)$ at the discretized instants t_j, for $j = 1, \ldots, N_t$. Moreover, $\{s_j(t)\}_{j=1,\ldots,N_t}$ is the basis of hat functions for time discretization. Substituting (9) in (4), control law is defined $\forall (x, y, t) \in \Omega \times T^*$ as:

$$u(x, y, t) = \sum_{i=1}^{4} \sum_{j=1}^{N_t} u_{ij} s_j(t) \mathbf{1}_{\mathcal{D}_i}(x, y) \tag{10}$$

Based on (10), $u(x, y, t)$ is perfectly determined by the knowledge of $\mathbf{u} = [u_{ij}]_{\substack{i=1,\ldots,4 \\ j=1,\ldots,N_t}}$. Criterion J is minimized by an iterative descent algorithm: $J(\psi; \mathbf{u}^{n+1}) < J(\psi; \mathbf{u}^n)$. At each new iteration $n + 1$, $\mathbf{u}$ is modified according to the values obtained at the previous iteration n as:

$$\begin{aligned} &\mathbf{u}^{n+1} = \mathbf{u}^n - \gamma^n \mathbf{d}^n \\ &u_{ij}^{n+1} = u_{ij}^n - \gamma^n d_{ij}^n \quad \forall i = 1, \ldots, 4,\ \forall j = 1, \ldots, N_t \end{aligned} \tag{11}$$

where γ^n is the descent depth and $\mathbf{d}^n$ is the descent direction such that:

$$\begin{aligned} &\mathbf{d}^n = -\nabla J^n + \beta^n \mathbf{d}^{n-1} \\ &d_{ij}^n = -\frac{\partial J}{\partial u_{ij}^n} + \beta^n d_{ij}^{n-1} \quad \forall i = 1, \ldots, 4,\ \forall j = 1, \ldots, N_t \end{aligned} \tag{12}$$

with $\beta^0 = 0$ and $\beta^n = \dfrac{\|\nabla J^n\|_F^2}{\|\nabla J^{n-1}\|_F^2}$, $\forall n \geq 1$ ($\|.\|_F$ is the Frobenius norm). At each new iteration of the minimization

algorithm, it is crucial to evaluate the cost function value $J^n = J(\psi^n; u)$, the descent direction $\mathbf{d}^n$ (based on the cost function gradient ∇J^n), and the descent depth γ^n. In such a context, three well-posed problems must be solved.

B. *Direct problem*

Direct problem (5)-(7) is solved on $\Omega \times T^*$ considering $u^n(x, y, t)$. Then, once error function ψ^n is numerically obtained, cost function $J(\psi^n; u^n)$ defined in (8) is estimated.

C. *Sensitivity problem*

The sensitivity function is defined $\forall (x, y, t) \in \Omega \times T^*$ as:

$$\delta\psi = \lim_{\varepsilon \to 0} \frac{\psi^+(x, y, t; u) - \psi(x, y, t; u)}{\varepsilon} \tag{13}$$

where $\psi^+(x, y, t; u) = \psi(x, y, t; u^+)$ results from the control variation $u^+ = u + \varepsilon\delta u$, and is the solution of the following PDE system on $\Omega \times T^*$:

$$\rho C \frac{\partial \psi^+}{\partial t} - \lambda \Delta \psi^+ = \lambda \Delta \theta_{target} + \frac{-h(\psi^+ - \psi_0) + u^+}{e} \tag{14}$$

$$\psi^+(x, y, 0) = \psi_0(x, y) \quad \text{on } \Omega \tag{15}$$

with the Neumann boundary condition:

$$-\lambda \frac{\partial \psi^+}{\partial \vec{n}} = 0 \quad \text{on } \Gamma \times T^* \tag{16}$$

Subtracting (5)-(7) from (14)-(16) respectively, and considering (13), sensitivity function $\delta\psi^n$ at iteration n is the solution of the following sensitivity problem:

$$\rho C \frac{\partial \delta\psi}{\partial t} - \lambda \Delta \delta\psi = \frac{-h\delta\psi + \delta u}{e} \qquad \text{on } \Omega \times T^* \tag{17}$$

$$\delta\psi(x, y, 0) = \delta\psi_0(x, y) = 0 \qquad \text{on } \Omega \tag{18}$$

with the Neumann boundary condition:

$$-\lambda \frac{\partial \delta\psi}{\partial \vec{n}} = 0 \qquad \text{on } \Gamma \times T^* \tag{19}$$

Descent depth is defined by:

$$\gamma^n = \arg\min_{\gamma \in \mathbb{R}} J(\mathbf{u}^{n+1}) = \arg\min_{\gamma \in \mathbb{R}} J(\mathbf{u}^n - \gamma \mathbf{d}^n) \tag{20}$$

$$= \arg\min_{\gamma \in \mathbb{R}} \frac{1}{2} \sum_{i=1}^{9} \psi(A_i, t_f^*; \mathbf{u}^n - \gamma \mathbf{d}^n)^2 \tag{21}$$

Equation (20) implies that $\dfrac{\partial J(\mathbf{u}^n - \gamma \mathbf{d}^n)}{\partial \gamma} = 0$. Utilizing it in the Taylor approximation for (21), this yields:

$$\gamma^n = \frac{\displaystyle\sum_{i=1}^{9} \psi(A_i, t_f^*; \mathbf{u}^n) \delta\psi_{\mathbf{d}^n}(A_i, t_f^*; \mathbf{u}^n)}{\displaystyle\sum_{i=1}^{9} (\delta\psi_{\mathbf{d}^n}(A_i, t_f^*; \mathbf{u}^n))^2} \tag{22}$$

where $\delta\psi_{\mathbf{d}^n}$ is the variation of ψ induced by the variation of the control in the descent direction $\mathbf{d}^n$. Thus sensitivity problem resolution leads to the numerical evaluation of the descent depth γ^n.

D. *Adjoint problem*

Define the Lagrangian at iteration n as:

$$\mathcal{L} = J + \int_{T^*} \int_{\Omega} \left(\rho C \frac{\partial \psi^n}{\partial t} - \lambda \Delta \psi^n - \lambda \Delta \theta_{target} - \frac{-h(\psi^n - \psi_0) + u^n}{e} \right) \varphi^n \, dxdydt \tag{23}$$

where $\varphi^n(x, y, t)$ is its multiplier. Lagrangian differential is:

$$\delta\mathcal{L} = \frac{\partial \mathcal{L}}{\partial \varphi^n} \delta\varphi^n + \frac{\partial \mathcal{L}}{\partial \psi^n} \delta\psi^n + \frac{\partial \mathcal{L}}{\partial u^n} \delta u^n$$

If φ^n is fixed, then $\dfrac{\partial \mathcal{L}}{\partial \varphi^n} \delta\varphi^n = 0$. Note that the sum in (8) could be reformulated as an integral thanks to the Dirac distribution function $\delta_{A_i}(x, y)$ related to the pointwise sensor A_i. Indeed, it is rewritten as:

$$J(\psi^n; u^n) = \frac{1}{2} \sum_{i=1}^{9} \int_{\Omega} \psi(x, y, t_f^*; u^n)^2 \delta_{A_i}(x, y) dxdy$$

Substituting it in (23), thus

$$\frac{\partial \mathcal{L}}{\partial \psi^n} \delta\psi^n = \sum_{i=1}^{9} \int_{\Omega} \psi^n(x, y, t_f^*) \delta\psi^n(x, y, t_f^*) \delta_{A_i}(x, y) dxdy + I_1 + I_2 + \int_{T^*} \int_{\Omega} \frac{h\delta\psi^n}{e} \varphi^n \, dxdydt$$

where

- $I_1 = \displaystyle\int_{T^*} \int_{\Omega} \left(\rho C \frac{\partial \delta\psi^n}{\partial t} \right) \varphi^n \, dxdydt$
- $I_2 = -\displaystyle\int_{T^*} \int_{\Omega} \lambda \Delta \delta\psi^n \varphi^n \, dxdydt$

Integrating I_1 and I_2 by parts, and utilizing the sensitivity problem initial and boundary conditions (18)-(19), it comes:

$$\begin{aligned}
&\frac{\partial \mathcal{L}}{\partial \psi^n} \delta\psi^n = \\
&\int_{\Omega} \left(\sum_{i=1}^{9} \psi^n(., t_f^*) \delta_{A_i}(.) + \rho C \varphi^n(., t_f^*) \right) \delta\psi^n(., t_f^*) \, dxdy \\
&- \int_{T^*} \int_{\Omega} \left(\rho C \frac{\partial \varphi^n}{\partial t} + \lambda \Delta \varphi^n - \frac{h\varphi^n}{e} \right) \delta\psi^n \, dxdydt \\
&- \int_{T^*} \int_{\Gamma} \delta\psi^n \lambda \frac{\partial \varphi^n}{\partial n} \, dxdydt
\end{aligned}$$

with the notation $(.) = (x, y)$. Lagrangian multiplier φ^n is fixed in order to satisfy $\dfrac{\partial \mathcal{L}}{\partial \psi^n} \delta\psi^n = 0$. Therefore, the following (backward) adjoint problem (24)-(26) is obtained such that on $\Omega \times T^*$:

$$\rho C \frac{\partial \varphi^n}{\partial t} + \lambda \Delta \varphi^n = \frac{h\varphi^n}{e} \tag{24}$$

and $\forall (x, y) \in \Omega$:

$$\varphi^n(x, y, t_f^*) = -(\rho C)^{-1} \sum_{i=1}^{9} \psi^n(x, y, t_f^*) \delta_{A_i}(x, y) \tag{25}$$

with the Neumann boundary condition on $\Gamma \times T^*$:

$$-\lambda \frac{\partial \varphi^n}{\partial \vec{n}} = 0 \tag{26}$$

Consequently,

$$\delta \mathcal{L} = \frac{\partial \mathcal{L}}{\partial u^n} \delta u^n = -\int_{T^*} \int_{\Omega} \delta u^n \frac{\varphi^n}{e} \, dxdydt \tag{27}$$

If ψ^n is solution of the direct problem (5)-(7), then $\delta \mathcal{L} = \delta J$. Using it in (27), this implies:

$$\begin{aligned} \delta J = \frac{\partial J}{\partial u^n} \delta u^n &= \sum_{i=1}^{4} \sum_{j=1}^{N_t} \frac{\partial J}{\partial u_{ij}^n} \delta u_{ij}^n \\ &= -\int_{T^*} \int_{\Omega} \delta u^n \frac{\varphi^n}{e} \, dxdydt \\ &= -\sum_{i=1}^{4} \sum_{j=1}^{N_t} \int_{T^*} \int_{\mathcal{D}_i} \delta u_{ij}^n s_j(t) \frac{\varphi^n}{e} dxdydt \end{aligned}$$

Thus for all $i = 1, \ldots, 4$ and $j = 1, \ldots, N_t$

$$\frac{\partial J}{\partial u_{ij}^n} = -\int_{T^*} \int_{D_i} \frac{\varphi^n(x,y,t)}{e} s_j(t) \, dxdydt \tag{28}$$

Therefore, the adjoint problem resolution led to the numerical evaluation of the cost function gradient at iteration n. Consequently, the descent direction in (12) is deduced.

V. Algorithm

The CGM iteratively relies on the three well-posed problems:

- direct problem (5)-(7) for cost function (criterion) estimation in (8)
- adjoint problem (24)-(26) for computing the criterion gradient in (28)
- sensitivity problem (17)-(19) for obtaining the descent depth in (22)

The algorithm implemented for this paper is as follows:

➢ ***Step*** 1 (*Initialization*)
- at iteration $n = 0$, set the control $u^0(x, y, t) = 0$

➢ ***Step*** 2 (*Direct problem*)
- solve the direct problem (5)-(7) with control u^n and deduce J according to (8)
  - if $J \leq J_{stop}$ (*the stopping criteria*) or $n = n_{max}$ (*the maximum number of iterations*), stop the CGM and consider u^n as the unknown approximation
  - if not, move to *Step* 3

➢ ***Step*** 3 (*Adjoint problem*)
- solve the adjoint problem (24)-(26)
- calculate $\nabla J^n = \left[\frac{\partial J}{\partial u_{ij}^n} \right]_{\substack{i=1,\ldots,4 \\ j=1,\ldots,N_t}}$ in (28)
- deduce the descent direction d^n in (12)

➢ ***Step*** 4 (*Sensitivity problem*)
- solve the sensitivity problem (17)-(19)
- deduce the descent depth γ^n in (22)

➢ ***Step*** 5 (*Control update*)
- update the control $u^{n+1} = u^n - \gamma^n d^n$ in (11)
- increment the iteration $n = n+1$ and return to *Step* 2

Usually J_{stop} is a key parameter in the CGM regularization property. For "classical" identification purposes (see for example [5], [10], [11], [12]), observations are noisy disturbed (noises are mainly induced by measurement errors). In such a context, if J_{stop} is too small, the algorithm could not converge or will converge towards an identified control which is critically affected by the measurement noise. However if J_{stop} is too large, identification process is not accurate and leads to an erroneous estimation. In the specific control of this communication, disturbances on the desired target are neglected. Then J_{stop} is only related to the mean square deviation between the obtained state and the desired target. It is therefore chosen according to our knowledge of magnitude orders of the target temperature.

VI. Stabilization in finite time: numerical results

In the following, simulation results are attained with a final time $t_f^* = 300$ s and a stopping criterion $J_{stop} = 1$. The cost function minimization algorithm implemented under the condition $J \leq J_{stop}$ is well executed, where the corresponding CPU time took about 10 minutes for 15 iterations (see fig. 4). Table III demonstrates the error function for the 9 sensors at the time t_f^*. The control identification strategy is quite relevant as the controlled error function absolute mean is 0.36 °C, compared to 21.4 °C for the uncontrolled one. In fig. 5, temperature variation is illustrated for all the sensors on $T^* = [0, 300]$. Its evolution without control (dotted line) and the desired target (dashed line) respectively correspond to those obtained in fig. 3 at $t = 300$ s and $t = 3600$ s. For each sensor, the controlled temperature (solid line) converges at $t = 300$ s towards the desired target. Last but not least, the identified control laws (leading to significant results in table III and fig. 5) are shown in fig. 6. It is crucial to recognize that negative values play a vital role in stabilizing the system close to the desired target, particularly following significant positive heating fluxes inducing rapid temperature increase.

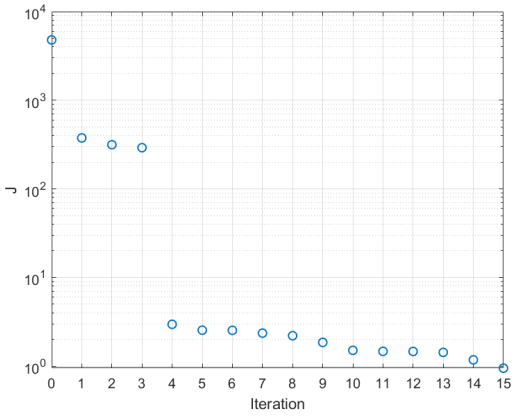

Fig. 4: Cost function evolution versus iteration.

TABLE III: Error function $\psi(A_i, t_f^*)$

	A_1	A_2	A_3	A_4	A_5
without control	-7.82	-8.42	-26.92	-14	-24.42
with control	-0.9	0.63	-0.09	-0.16	0.57
	A_6	A_7	A_8	A_9	
without control	-28.12	-24.1	-24.84	-33.92	
with control	0.35	-0.07	-0.41	-0.02	

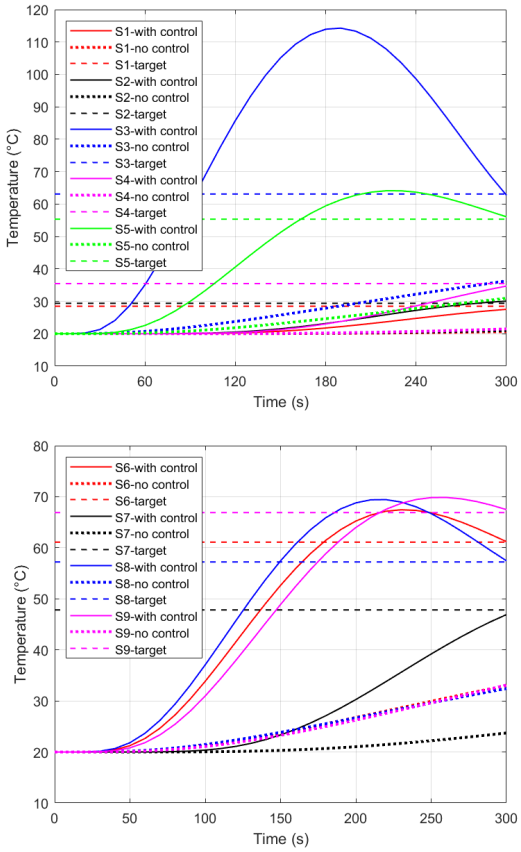

Fig. 5: Temperature evolution at S_i (Sensors A_i): controlled versus uncontrolled.

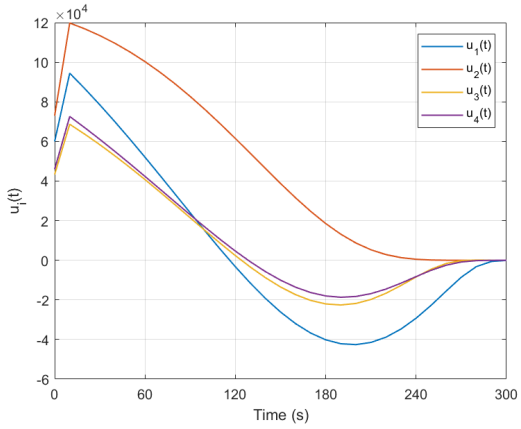

Fig. 6: Controllers variation.

VII. Concluding remarks

This paper highlights the interest of the conjugate gradient regularization method (governed by PDEs) to efficiently deal with ill-posed inverse identification problems and achieve finite-time stabilization in 2D thermal geometries. The aim is not only to extend recent research on control mainly focused on 1D domains (see [1], [2]), but also to go beyond simulations concerned with parametric identifications (see [5], [12]) and provide control synthesis strategies different from those proposed in [3], [7], [8]. This is particularly interesting for non-academic situations, where no theoretical results could be considered (these being generally obtained with reductive assumptions). Stabilization in finite time provides a comprehensive interpretation of the advantages of the conjugate gradient method and a significant insight into various scenarios. In particular, the method shows promise for temperature control in complex 3D domains, without the limitations imposed by thin plate thickness. In addition, the application extends to the control of moving disks and the identification of trajectories for rejecting forced moving disturbances, where this could require fewer controllers. A necessary adaptation by a quasi-online determination of control laws (in small sliding intervals in real time) would make it possible to reduce CPU time.

References

[1] Azar T., et al. "Quasi-Online Disturbance Rejection for Nonlinear Parabolic PDE using a Receding Time Horizon Control." 2021 *European Control Conference (ECC)*. IEEE, 2021.

[2] Azar T., Perez L., Prieur C., Moulay E., & Autrique L., (2020). Stabilization and disturbances rejection using internal actuator for the heat equation, *Controlo 2020, Bragança, Portugal, 1-3 july 2020*.

[3] Bárcena-Petisco, Jon Asier. "Null controllability of the heat equation in pseudo-cylinders by an internal control." ESAIM: Control, *Optimisation and Calculus of Variations* 26 (2020): 122.

[4] Bao G., Coron J. M., & Li, T. (Eds.). (2019). *Control and Inverse Problems for Partial Differential Equations* (Vol. 22). World Scientific.

[5] Beddiaf S., Perez L., Autrique L., & Jolly J. C. (2014). Simultaneous determination of time-varying strength and location of a heating source in a three-dimensional domain. *Inverse Problems in Science and Engineering, 22*(1), 166-183.

[6] Gaye O., Moulay E., Brémond S., Autrique L., Nouailletas R., Artaud J. F., & Orlov Y. (2013). Robust stabilization of the current profile in Tokamak plasmas using sliding mode approach in infinite dimension. *Control Engineering Practice, 21*(10), 1350-1358.

[7] Orlov Y., Perez L., Gomez O., & Autrique L. (2020). ISS output feedback synthesis of disturbed reaction–diffusion processes using non-collocated sampled-in-space sensing and actuation. *Automatica, 122*, 109257.

[8] Ou Yongsheng, Schuster E., (2009) "Model predictive control of parabolic PDE systems with dirichlet boundary conditions via galerkin model reduction." *2009 American Control Conference*. IEEE, 2009.

[9] Ozisik M. N. (2018). *Inverse heat transfer: fundamentals and applications*. Routledge.

[10] Rouquette S., Autrique L., Chaussavoine C., & Thomas L. (2007). Identification of influence factors in a thermal model a plasma assisted chemical vapour deposition process, *Inverse Problems in Science and Engineering, 15*(5), 489-515.

[11] Vergnaud A., Perez L., Autrique L. (2020) "Adaptive selection of relevant sensors in a network for unknown mobile heating flux estimation." *IEEE Sensors Journal* 20.24 : 15133-15142.

[12] Vergnaud A., Beaugrand G., Gaye O., Perez L., & Autrique, L. (2014). "On-line identification of temperature-dependent thermal conductivity." *European Control Conference*, 2139-2144.